$\eta \to \gamma\gamma$ Decay Width via the Primakoff Cross Section

T. E. Rodrigues,[1] J. D. T. Arruda-Neto,[1,2] J. Mesa,[3] C. Garcia,[4] K. Shtejer,[1,4] D. Dale,[5] I. Nakagawa,[6] and P. L. Cole[5]

[1]Physics Institute, University of São Paulo, P. O. Box 66318, CEP 05315-970, São Paulo, Brazil

[2]FESP-São Paulo Engineering College, São Paulo, Brazil

[3]Department of Physics and Biophysics, UNESP, Botucatu, Brazil

[4]Center of Applied Studies for Nuclear Developments (CEADEN), Havana, Cuba

[5]Department of Physics, Idaho State University, Pocatello Idaho, 83209, USA

[6]RIKEN 2-1 Hirosawa, Wako, Saitama 351-0198, Japan

(Received 26 April 2007; revised manuscript received 28 January 2008; published 3 July 2008)

Incoherent η photoproduction in nuclei is evaluated at forward angles within 4 to 9 GeV using a multiple scattering Monte Carlo cascade calculation with full η-nucleus final-state interactions. The Primakoff, nuclear coherent and nuclear incoherent components of the cross sections fit remarkably well previous measurements for Be and Cu from Cornell, suggesting a destructive interference between the Coulomb and nuclear coherent amplitudes for Cu. The inelastic background of the data is consistently attributed to the nuclear incoherent part, which is clearly not isotropic as previously considered in Cornell's analysis. The respective Primakoff cross sections from Be and Cu give $\Gamma_{\eta\to\gamma\gamma} = 0.476(62)$ keV, where the quoted error is only statistical. This result is consistent with the Particle Data Group average of 0.510(26) keV and in sharp contrast ($\sim 50\%$) with the value of 0.324(46) keV obtained at Cornell.

DOI: 10.1103/PhysRevLett.101.012301 PACS numbers: 25.20.Lj, 12.40.Vv, 13.40.Hq, 24.10.Lx

Next-to-leading order calculations based on chiral perturbation theory (ChPT) [1,2] have shown an enhancement of the $\pi^0 \to \gamma\gamma$ decay width by about 4% with respect to the chiral axial anomaly prediction [3], mostly associated with the isospin breaking induced mixing of the pure SU(3) states η and η'. Another small correction to the leading order $\pi^0 \to \gamma\gamma$ amplitude was recently attributed to excited mesonic states using QCD sum rules [4], making salient the need for accurate measurements of both $\Gamma_{\pi^0\to\gamma\gamma}$ and $\Gamma_{\eta\to\gamma\gamma}$, since the later is a necessary input to obtain $\Gamma_{\pi^0\to\gamma\gamma}$ beyond the chiral anomaly [1,2,4]. The $\eta \to \gamma\gamma$ decay width has been measured in two-photon experiments [5] and via the Primakoff effect [6] at Cornell [7], leading to extremely discrepant results. While the two-photon measurements are consistent with each other, Cornell's measurement [0.324(46) keV] is severely below their average, and was recently excluded from the Particle Data Group (PDG) world average [0.510(26) keV] [8]. Such a long-standing issue is strong evidence of a misunderstanding of the hadronic inelastic background in the Cornell analysis.

A renewed interest in the Primakoff method appeared with the advent of the PrimEx Collaboration at the Jefferson Laboratory, which will provide a more precise measurement of $\Gamma_{\pi^0\to\gamma\gamma}$[9]. Furthermore, high precision η and η' photoproduction experiments are strongly encouraged by the forthcoming 12 GeV upgrade of the electron beam, demanding reliable methods for the accurate delineation of the nuclear background.

The approaches developed so far for incoherent η photoproduction from nuclei are restricted to ~ 1 GeV, where the contribution from the $S_{11}(1535)$ resonance largely dominates. The final-state interactions (FSI) of the η mesons are taken into account either using optical potentials [10], the quantum molecular dynamics (QMD) model of Ref. [11], or the Boltzmann-Uehling-Uhlenbeck (BUU) transport model [12]. Obviously, these important theoretical developments are not suitable to describe incoherent production at higher energies.

In this Letter, we present for the first time a consistent solution for the puzzling scenario of $\Gamma_{\eta\to\gamma\gamma}$ from Cornell using the multicollisional intranuclear cascade model MCMC [13–15] to describe the nuclear background. The Monte Carlo (MC) method takes into account incoherent η photoproduction from nuclei at forward angles within 4 to 9 GeV, including η-nucleus FSI via a multiple scattering framework.

The forward angle η photoproduction cross section is assumed to be in the form [16–18]

$$\frac{d\sigma}{d\Omega} = |T_P + e^{i\varphi}T_{NC}|^2 + |T_{NI}|^2, \quad (1)$$

where T_P, T_{NC}, and T_{NI} are the Primakoff (P), nuclear coherent (NC), and nuclear incoherent (NI) amplitudes, respectively, with φ representing the P-NC phase shift.

The Coulomb amplitude is the sum of the amplitudes from the protons [6], such that

$$T_P = [8\alpha Z^2\Gamma_{\eta\to\gamma\gamma}]^{1/2}\left(\frac{\beta}{\mu}\right)^{3/2}\frac{k^2}{Q^2}\tilde{F}_C(k,\theta)\sin\theta, \quad (2)$$

where $\alpha = 1/137$, Z is the atomic number, k the photon energy, Q the four momentum transfer, $\tilde{F}_C(k,\theta)$ the Coulomb form factor (FF) including η-nucleus FSI; with $\Gamma_{\eta\to\gamma\gamma}$, β, μ, and θ representing the decay width, velocity, mass, and production angle of the η meson, respectively.

The NC amplitude is given by

$$T_{\rm NC} = A\tilde{F}_{\rm NC}(k,\theta)L\sin\theta, \tag{3}$$

where A is the nucleus mass, $\tilde{F}_{\rm NC}(k,\theta)$ the strong FF taking into account FSI, and $L\sin\theta$ the spin-nonflip nucleon amplitude. Such amplitude is not known precisely at our energies of interest, and we adopted $L = 4k$[7].

The NI cross section is written as [18] (neglecting FSI)

$$|T_{\rm NI}|^2 = Af(k,\theta)|T_n^s|^2 \equiv Af(k,\theta)\frac{d\sigma_n^s}{d\Omega}, \tag{4}$$

where $f(k,\theta)$ accounts for the Pauli-blocking and T_n^s is the total amplitude for η photoproduction from the nucleon T_n without the Coulomb part.

The elementary amplitude T_n is calculated for $k \gtrsim 4$ GeV and $\theta \ll 1$ using t-channel helicity amplitudes F_i[14,19]:

$$|T_n|^2 = \frac{p_*^2}{\pi}\frac{d\sigma_n}{dt} = \frac{p_*^2}{32\pi^2}\left[F_2^2 + \frac{F_3^2}{4m_N^2} - (t+\Delta^2)\left(\frac{F_1^2}{4m_N^2} + \frac{F_3^2}{16m_N^4} + \frac{F_1F_3}{2m_N}\frac{1}{p_*\sqrt{s}}\right) - \frac{t+\Delta^2}{p_*\sqrt{s}}\left(F_2 - \frac{F_3}{2m_N}\right)\left(\frac{F_1}{2} - \frac{\sqrt{s}}{24p_*}F_2 + \frac{4p_* - 5\sqrt{s}}{16m_Np_*}F_3\right)\right], \tag{5}$$

where p_* is the meson momentum in the center of mass of the s-channel, m_N the nucleon mass, Δ the longitudinal momentum transfer ($\frac{\mu^2}{2k_*}$); with s and t being the Mandelstam variables.

So, using the Regge model with Reggeon cuts from Refs. [20,21], we may write the t-channel helicity amplitudes assuming ω, ρ, and b1 meson exchanges (VMD). Consequently, adding constructively the Coulomb contribution F_1^C, the natural parity exchange amplitudes (F_1 and F_3) and the b1 contribution (F_2) become: $F_1 \to F_1^\rho + F_1^\omega + F_1^{\rm cut} + F_1^C$, $F_2 \to F_2^{\rm b1} + F_2^{\rm cut}$, and $F_3 \to F_3^\rho + F_3^\omega + F_3^{\rm cut}$. The amplitudes $F_1^{\rho,\omega}$, $F_1^{\rm cut}$, F_1^C, and $F_3^{\rm cut}$ were taken from Ref. [14] with

$$F_2^{\rm b1}(s,t) = ta_{\rm b1}\alpha_{\rm b1}(t)(\alpha_{\rm b1}(t)+1)(\alpha_{\rm b1}(t)+2)(\alpha_{\rm b1}(t)+3) \times \frac{1-e^{-i\pi\alpha_{\rm b1}(t)}}{\sin[\pi\alpha_{\rm b1}(t)]}\left(\frac{s-u}{s_0}\right)^{\alpha_{\rm b1}(t)-1}, \tag{6}$$

$$F_2^{\rm cut}(s,t) = \frac{\sqrt{2}}{m_N}\gamma_3^{\rm cut}\frac{1-e^{-i\pi\alpha(0)}}{\sin[\pi\alpha(0)]}\left(\frac{s}{s_0}\right)^{\alpha(0)-1}\frac{e^{at}}{\ln(\frac{s}{s_0})}, \tag{7}$$

and

$$F_3^{\rho,\omega}(s,t) = \frac{2\sqrt{2}}{m_N}t\gamma_3^{\rho,\omega}\frac{1-e^{-i\pi\alpha(t)}}{\sin[\pi\alpha(t)]}\alpha(t)[1+\alpha(t)][2+\alpha(t)]\left(\frac{s}{s_0}\right)^{\alpha(t)-1}. \tag{8}$$

The Regge trajectories were taken as $\alpha_{\omega,\rho}(t) = \alpha(t) = 0.39 + 1.0t$ and $\alpha_{\rm b1}(t) = -0.342 + 0.9t$ with $s_0 = 1$ GeV^2 and $u = 2m_N^2 + 2\mu^2 - t - s$. The coupling constants $\gamma_1^\rho + \gamma_1^\omega = -0.229K\sqrt{\mu{\rm b}}$ and $\gamma_3^\rho + \gamma_3^\omega = 0.130$ K$\sqrt{\mu{\rm b}}$ were taken from Ref. [21]. The other parameters, such as: $K = 184(24)$, $\gamma_1^{\rm cut} = -149.1(23)\sqrt{\mu{\rm b}}$ (see Ref. [14]), $\gamma_3^{\rm cut} = 7.6(12)\frac{\sqrt{\mu{\rm b}}}{\rm GeV}$, $a = 1.976(26)$ GeV^{-2}, and $a_{\rm b1} = 69(13)\frac{\sqrt{\mu{\rm b}}}{\rm GeV}$ were obtained by fitting the available data [21–23], where we have used $\Gamma_{\eta\to\gamma\gamma} = 0.510$ keV. The proposed Regge model for $\frac{d\sigma_n}{dt}$ is presented in Fig. 1, reproducing quite reasonably the available data ($\chi^2/n.d.f. = 61.76/44$).

The shapes for the P and NC components of Eq. (1) were taken from Cornell's analysis [7] to assure that the only difference between Cornell's and this approach is the inelastic part (NI). Such contribution was assumed to be isotropic, energy independent, and proportional to $A^{3/4}$ in Cornell's analysis and is more deeply investigated in this work.

The calculation of the FSI in NI η photoproduction is performed using an improved version of the MCMC model. The model consists of a relativistic and time-dependent multicollisional algorithm which incorporates: (i) the elementary η photoproduction [Eq. (5)], (ii) realistic momentum distributions for light nuclei [24], (iii) a nonstochastic Pauli-blocking mechanism during multiple ηN scatterings, and (iv) photon shadowing effects via a VMD

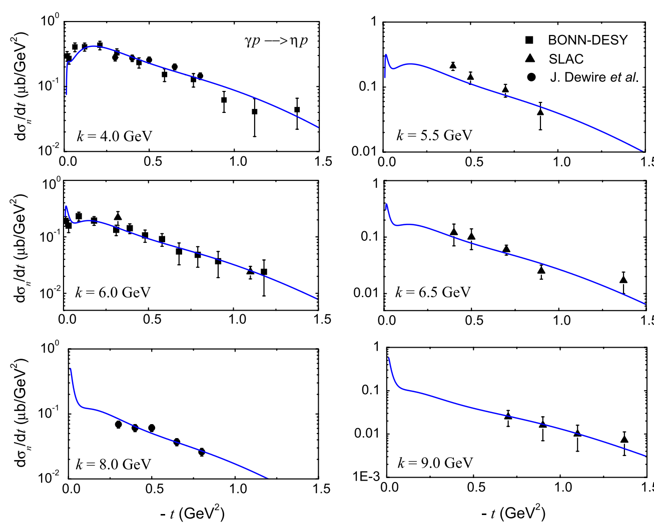

FIG. 1 (color online). Differential cross section for η photoproduction on the proton. The solid lines represent our Regge model including the Coulomb amplitude. The data points are from [21] (squares), [22] (triangles), and [23] (circles).

model [25]. The MCMC cascade also presents some advantages in comparison with other approaches—such as the integral formalism of Glauber [17]—since it includes local density fluctuations, meson energy losses, and NN correlations during secondary scatterings. The total ηN cross section was assumed to be the average $(\sigma_{\pi^+ p} + \sigma_{\pi^- p})/2$, with the later being given by Ref. [26]. The details of the calculations will be subject of a forthcoming paper [27].

The result of the NI cross section for Be at $k = 8.5$ GeV is presented in Fig. 2. The solid line is the PWIA ($A \frac{d\sigma_n^s}{d\Omega}$), and the dashed line includes the effect of Pauli-blocking [Eq. (4)]. The result taking into account FSI is obtained after running the cascade model with (dashed-dotted) and without (dotted) the shadowing effect.

Because of the absence of absolute cross section measurements of η photoproduction on nuclei, we restrict our analysis to the description of the η yields obtained for Be and Cu at Cornell [7] (The U data is not included due to inadequate angular resolution to disentangle the P and NC components unambiguously). With this approach, we may write the number of η events at a given angular bin $n(\theta)$ in terms of *shape factors* for the three components of the cross section, herein denoted $S_{\rm P}$, $S_{\rm NC}$, and $S_{\rm NI}$ [28]:

$$n(\theta) = a_{\rm P} S_{\rm P}(\theta) + a_{\rm NC} S_{\rm NC}(\theta) + a_{\rm NI} S_{\rm NI}(\theta) + 2\sqrt{a_{\rm P} a_{\rm NC}} \cos\varphi \sqrt{S_{\rm P}(\theta) S_{\rm NC}(\theta)}, \quad (9)$$

where $a_{\rm P}$, $a_{\rm NC}$, $a_{\rm NI}$, and φ are constants to be determined by fitting Be and Cu data simultaneously. The shapes of $S_{\rm P}$ and $S_{\rm NC}$ were taken from Cornell's analysis [7] to make salient our concentrated effort on the incoherent shape $S_{\rm NI}$. Furthermore, Cornell's shapes include angular resolution effects, which are very relevant for $S_{\rm P}$ due to the sharp Primakoff peak. The shapes of $S_{\rm NI}$ were then calculated neglecting angular resolution effects and folding the theoretical cross sections, calculated from 8 to 9 GeV in 100 MeV steps, with a flat bremsstrahlung spectrum. This procedure was employed since only high energy mesons ($8.05 \lesssim E_\eta \lesssim 9.0$ GeV) satisfy the Cornell kinematics [7]. Also, another MC algorithm was used to simulate the $\eta \to \gamma\gamma$ decay taking into account Cornell's kinematics and geometry [7].

Several approaches were used to fit Cornell's data. First, a five parameter fitting ($a_{\rm P}$, $a_{\rm NC}$, $a_{\rm NI}^{\rm Be}$, $a_{\rm NI}^{\rm Cu}$, and φ) was tried. Next, a six parameter fitting was also tried taking two different phase shifts. Both analyses lead to reasonable statistics ($\frac{\chi^2}{n.d.f.} \sim 1.3$) but imaginary phase shifts. Consequently, a seven parameter fitting was performed assuming two different $a_{\rm NC}$ parameters for Be and Cu, leading to improved statistics ($\frac{\chi^2}{n.d.f.} \sim 1.02$) and physical phase shifts. Additional fittings for fixed phase shifts were also performed. Table I summarizes our fittings, where the first line presents our seven parameter fitting, herein denoted main result. The parameters $a_{\rm P}$ and $a_{\rm NC}$ were obtained using the ratio of Primakoff and NC events from this and Cornell's analysis and the fitted parameters from Cornell for the same dataset (second line of Table I from Ref. [7]). The $a_{\rm P}$ and $a_{\rm NC}$ parameters of the main result are strongly correlated both for Be($\rho_{a_{\rm P}, a_{\rm NC}} = 0.46$) and Cu($\rho_{a_{\rm P}, a_{\rm NC}} = 0.67$). Furthermore, the $a_{\rm NC}$ parameters for Cu vary by a factor of almost 4 assuming constructive ($\varphi = 0$) and zero ($\varphi = \frac{\pi}{2}$) interference. This complicated scenario is attributed to the big overlap between $S_{\rm P}$ and $S_{\rm NC}$ for intermediate and heavy nuclei due to a FF effect, without adequate angular resolution from the experiments performed so far. Additionally, these strong correlations provide clear evidences for the discrepancy in the value of $\Gamma_{\eta\to\gamma\gamma}$ obtained at Cornell after averaging the results from Be, Al, Cu, Hg, and U, making salient the advantage of using light nuclei for similar measurements within this kinematics.

Figure 3 shows our main result (left panel) and the $S_{\rm NI}$ shapes from Cornell and this work (right panel) obtained for Be, where one easily observes that the NI component fits the data remarkably well at larger angles. A similar

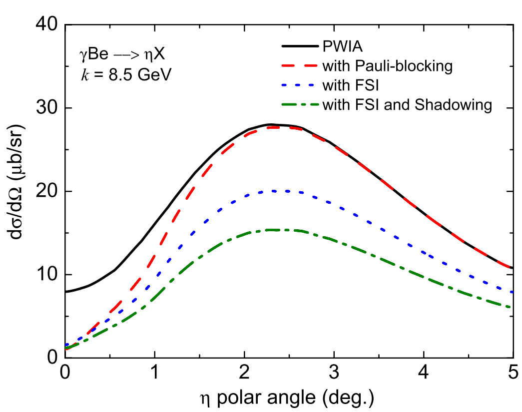

FIG. 2 (color online). NI η photoproduction cross section from Be at $k = 8.5$ GeV. The solid line is the PWIA, the dashed line includes the Pauli principle, and the dotted (dashed-dotted) lines take into account FSI without (with) photon shadowing.

TABLE I. Fitting results of Cornell's data from Be and Cu at $E_B = 9$ GeV. The first line represents our best χ^2 result for a seven parameter fitting. The three successive lines give our results for fixed phase shifts to elucidate the strong correlations between $a_{\rm P}$ and $a_{\rm NC}$.

	$a_{\rm P}$	$a_{\rm NC}$	$\frac{a_b \int n_b^{\rm Cornell}(\theta)d\theta}{a_{\rm NI}\int S_{\rm NI}^{\rm MCMC}(\theta)d\theta}$	φ(rad)	$\frac{\chi^2}{n.d.f}$
Be	0.476(62)	0.89(32)	0.957(70)	0.59(52)	$\frac{71.09}{70}$
Cu		6.3(13)	1.10(13)	1.88(19)	
Be	0.341(29)	1.07(15)	1.006(67)	0.0 (fixed)	$\frac{96.26}{72}$
Cu		0.93(27)	0.950(90)		
Be	0.470(26)	1.92(20)	1.079(83)	$\frac{\pi}{2}$ (fixed)	$\frac{112.93}{72}$
Cu		3.41(56)	1.03(11)		
Be	0.381(27)	1.42(17)	1.045(74)	1.0 (fixed)	$\frac{100.06}{72}$
Cu		1.54(38)	0.971(97)		

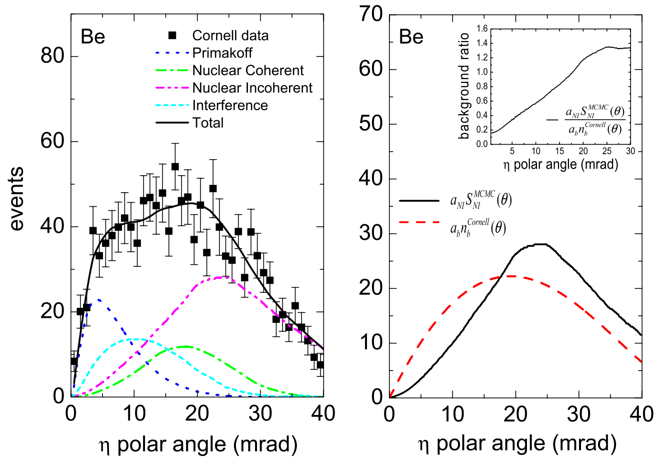

FIG. 3 (color online). Left panel: η photoproduction yield from Be at $E_B = 9$ GeV and fitted *shape factors* of the Primakoff (dotted line), NC (dashed-dotted line), NI (dashed-double-dotted line), and interference (short-dashed line) components of the total yield (solid line). The data points and the shapes of S_{P} and S_{NC} were taken from Ref. [7]. Right panel: S_{NI} *shape factors* from MCMC (solid line) and Cornell (dashed line) for Be. The insert presents the ratio $\frac{a_{\mathrm{NI}} S_{\mathrm{NI}}^{\mathrm{MCMC}}(\theta)}{a_{\mathrm{b}} n_{\mathrm{b}}^{\mathrm{Cornell}}(\theta)}$.

result is also obtained for Cu, where a destructive P-NC interference is highly favorable (see first line of Table I). Cornell's NI background is approximately 3 to 4 times higher than the MCMC prediction (see the insert) under the Primakoff peak ($\sim$5 mrad), since they have assumed an isotropic NI cross section. The MCMC background, however, is strongly suppressed at forward angles due to the exclusion principle. On the other hand, the total number of NI events from the MCMC and from Cornell are quite consistent with each other for all the fittings (third column of Table I). The final value of the decay width is extracted from our main result $\Gamma_{\eta\to\gamma\gamma} = 0.476(62)$ keV, where the quoted error represents a lower limit as it includes only the statistical error from the fitting.

In conclusion, a sophisticated calculation was developed to describe the hadronic inelastic background in Cornell's data of η photoproduction from Be and Cu at $E_B = 9$ GeV. Such reanalysis propitiated the extraction of $\Gamma_{\eta\to\gamma\gamma}$ via the Primakoff cross sections, providing a consistent explanation for the long-standing discrepancy between Cornell's data and the PDG average of 0.510 (26) keV. The destructive interference observed for Cu could be further investigated in high-resolution experiments, where a lower correlation between the fitted parameters should be expected. Additional measurements of η photoproduction on light nuclei and on the proton are highly recommended for a better understanding of the elementary amplitude, the ηN coupling constant in nuclear matter, and a more accurate determination of $\Gamma_{\eta\to\gamma\gamma}$ via the Primakoff effect.

We are indebted to Professor A. M. Bernstein for various illuminating discussions and to Professor O. Helene for reviewing our statistical considerations. We also thank the Brazilian agency FAPESP for the partial support of this work.

[1] J. L. Goity, A. M. Bernstein, and B. R. Holstein, Phys. Rev. D **66**, 076014 (2002).
[2] B. Ananthanarayan and B. Moussallam, J. High Energy Phys. 05 (2002) 052.
[3] J. S. Bell and R. Jackiw, Nuovo Cimento A **60**, 47 (1969); S. L. Adler, Phys. Rev. **177**, 2426 (1969).
[4] B. L. Ioffe and A. G. Oganesian, Phys. Lett. B **647**, 389 (2007).
[5] S. E. Baru *et al.*, Z. Phys. C **48**, 581 (1990); N. A. Roe *et al.*, Phys. Rev. D **41**, 17 (1990); D. A. Williams *et al.*, Phys. Rev. D **38**, 1365 (1988); W. Bartel *et al.*, Phys. Lett. B **160**, 421 (1985).
[6] H. Primakoff, Phys. Rev. **81**, 899 (1951).
[7] A. Browman *et al.*, Phys. Rev. Lett. **32**, 1067 (1974).
[8] W.-M. Yao *et al.* (Particle Data Group), J. Phys. G **33**, 1 (2006).
[9] http://www.jlab.org/primex/primex_notes/proposal_pac_33/proposal_pac_33.ps.
[10] M. Hedayati-Poor and H. S. Sherif, Nucl. Phys. A **740**, 309 (2004).
[11] T. Yorita *et al.*, Phys. Lett. B **476**, 226 (2000).
[12] J. Lehr, M. Post, and U. Mosel, Phys. Rev. C **68**, 044601 (2003).
[13] T. E. Rodrigues *et al.*, Phys. Rev. C **69**, 064611 (2004).
[14] T. E. Rodrigues *et al.*, Phys. Rev. C **71**, 051603(R) (2005).
[15] T. E. Rodrigues *et al.*, Braz. J. Phys. **36**, 1366 (2006).
[16] G. Morpurgo, Nuovo Cimento **31**, 569 (1964).
[17] G. Faldt, Nucl. Phys. **43**, 591 (1972).
[18] C. A. Engelbrecht, Phys. Rev. **133**, B988 (1964).
[19] A. Gasparian and S. Gevorkyan (private communication).
[20] M. Braunschweig *et al.*, Nucl. Phys. B **20**, 191 (1970).
[21] W. Braunschweig *et al.*, Phys. Lett. B **33**, 236 (1970).
[22] R. Anderson *et al.*, Phys. Rev. D **1**, 27 (1970).
[23] J. Dewire *et al.*, Phys. Lett. B **37**, 326 (1971).
[24] L. Lapikas, G. van der Steenhoven, L. Frankfurt, M. Strikman, and M. Zhalov, Phys. Rev. C **61**, 064325 (2000).
[25] T. H. Bauer, R. D. Spital, and D. R. Yennie, Rev. Mod. Phys. **50**, 261 (1978).
[26] J. R. Cudell *et al.*, Phys. Rev. D **65**, 074024 (2002).
[27] T. E. Rodrigues *et al.*, Nuclear incoherent photoproduction of pseudo-scalar mesons from 4 to 12 GeV (to be published).
[28] A different notation is employed in Ref. [7] for the Primakoff $[a_c n_c(\theta)]$, NC $[a_N n_N(\theta)]$, and NI $[a_{\mathrm{b}} n_{\mathrm{b}}(\theta)]$ components of Eq. (9).